International Journal of Engineering Applied Sciences and Technology, 2024
Vol. 8, Issue 12, ISSN No. 2455-2143, Pages 44-56
Published Online April 2024 in IJEAST (http://www.ijeast.com)

TRANSFER FUNCTION IDENTIFICATION AND CONTROL OF ETHYL ACETATE HYDROLYSIS IN A CSTR USING ASPEN HYSYS AND MATLAB

Mohamad Hassan Hamadelnil Deifalla
Department of Chemical Engineering
Sudan University of Science and Technology, Khartoum, Sudan

Gurashi Abdalla Gasmelseed
Department of Chemical Engineering
University of Science and Technology, Khartoum, Sudan

Adil Ali Mohammed
Department of Chemical Engineering
Karary University, Khartoum, Sudan

Abstract— **Cascade control strategy is used to maintain process conditions at their desired values by manipulating certain process variables to adjust the variables of interest. This paper presents cascade control for ethyl acetate hydrolysis with sodium hydroxide in a CSTR using Aspen HYSYS in dimentions of 1.5 m in diameter and 4.5 m in height. The dynamic-state simulation was used to determine the** behavior **of the** system **as a function of time system. MATLAB was used in identification of the system transfer functions, stability and response simulation. The ultimate gains for the control loop were determined using different methods: direct substitution, Routh-Hurwitz, Root-locus and Bode methods. The ultimate parameters for control loops showed that direct substitution method gave the highest gains: K_U = 267.661 for the secondary control loop while Routh- Hurwiz stability cirterion gave the highest gains: K_U = 3.17 for the primary control loop. Simulink was used to determine the ultimate parameters for secondary and primary loops. The controllers of the loops were tuned using Ziegler-Nichols techniques. In selecting the proper controller mode, the method was based on selecting the one that gives the best performance with respect to overshoot, rise time and settling time. Whereby, the PID controller showed the best performance for secondary and primary loops.**

Keywords— **Cascade Control, Ethyl Acetate Hydrolysis, CSTR, Transfer function identification, Tuning.**

I. INTRODUCTION

Many processes of industrial interest are difficult to control for their inherent nonlinear behavior presence of input constraints and lack of measurements [1-5]. Among these systems chemical processes have been widely studied and traditionally controlled using linear system analysis and design tools together with linearized models [6-8], or nonlinear methods based on linearization techniques [9-15]. However, the use of linear techniques is very limiting if the analyzed chemical process is highly nonlinear whereas nonlinear control design needs in general too much information about the process [1]. However, in some industrial applications cascade control improves the feedback control performance significantly [16].

International Journal of Engineering Applied Sciences and Technology, 2024
Vol. 8, Issue 12, ISSN No. 2455-2143, Pages 44-56
Published Online April 2024 in IJEAST (http://www.ijeast.com)

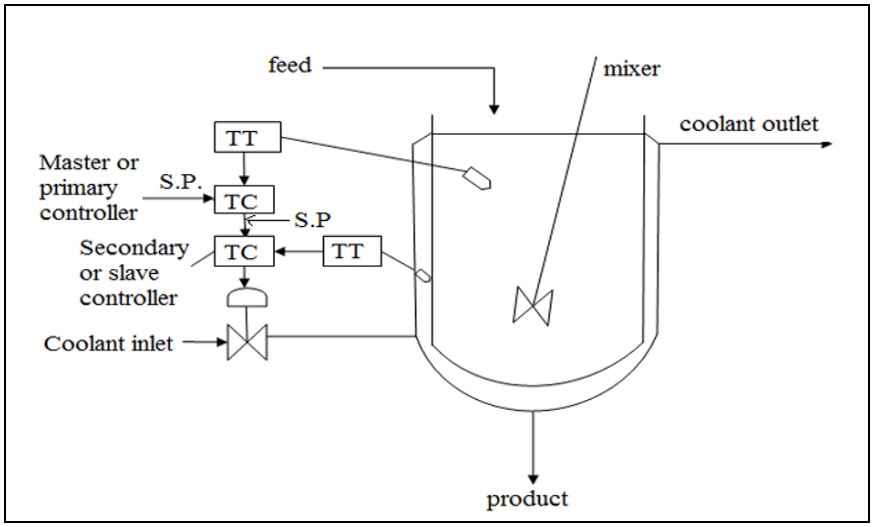

Fig. 1: Cascade Control of a CSTR [17, 18].

Cascase control strategy is consisting of one control element withtwo controllers, two sensors and two transmiters as shown in fig.1 [17].

Chemical reactors exhibit a challenging control problem due to their nonlinearity chaotic behavior and the presence of several stable and unstable equilibrium points. The uncertainty affecting the kinetic parameters is also not negligible: modeling of kinetic reactions is difficult and as a result the model mismatch may be significant [19]. If the controller design utilizes too much information the control performance may be severely degraded. Furthermore, most nonlinear control techniques assume that all state variables are measured or accurately estimated. In industrial practice the estimation of unmeasured state variables and unknown parameters are not a trivial problem.

Usually, only the temperatures and flow rates are easily measurable and although advanced methods for accurate measurement of the concentrations in a chemical reactor have been developed these have not been used frequently in industrial plants because of very high operating costs. Finally, the hard constraints imposed on the control input may adversely affect the efficiency of the controller and degrade the overall performance of the control system. In recent years there have been several pioneering modeling and simulation studies that have focused on saponification of ethyl acetate. Javinsky and Kadlec [20], investigated the time optimal control problem for jacket cooled for saponification reaction in a CSTR on an analog computer. Mungcharoen and Onifade [21], developed a mathematical model for investigating the chemical and physical processes for ethyl acetate hydrolysis in a PFR. They compared the simulated values of the outlet concentration, the outlet temperature, the residence time and conversion of sodium hydroxide with experiments. Djaeni et al. [22], developed a mathematical model for investigating the response and tuning of proportional (P), proportional integral (PI) and proportional integral derivative (PID) to maintain soap concentration in CSTR. They found the PID controller had the best response. Their model results were verified with experimental data, and they proved that simulation results satisfactorily fit for the experimental model. Mousa and Dawood [23], studied the saponification dynamics for identifying the system transfer function in CSTR. Their results showed that the multi input multi output system. Mousa and Dawood [24], investigated the CSTR control using PID, fuzzy logic and intelligent control strategies for saponification process. They concluded that the Fuzzy logic control shows better results according controllers performance. In recent years there have been several pioneering modeling and simulation studies that have focused on saponification of ethyl acetate. Türkşen et al. [25], modeled and analyzed the effects of operating parameters and to obtain the compromise process factor values for a continuous hydrolysis process. They optimized the conversion as 0.989 and the space-time as 6.4895 min^{-1}. Zare et al. [26], studied the kinetic modelling and simulation of hydrolysis of ethyl acetate in the presence of Sodium hydroxide in a plug flow reactor, Continues stirred tank reactor using Aspen Plus simulation Software. They found Plug flow reactors have a high volumetric unit conversion as the occurrence for side reactions are minimum. Deifalla [27], designed a conventional control strategy for ethyl acetate hydrolysis for CSTR. He obtained the system transfer functions using simulation approach, and designed a PID controller based on the best performance with respect to overshoot, rise time and settling time.

II. METHODOLOGY

1. Aspen HYSYS Simulation

The ethyl acetate hydrolysis by sodium hydroxide is shown as [28, 29]:

$$CH_3CO_2C_2H_5 + NaOH \rightarrow C_2H_5OH + CH_3CO_2Na \quad (1)$$

The reaction rate for the aforementioned reaction is given as [29]:

International Journal of Engineering Applied Sciences and Technology, 2024
Vol. 8, Issue 12, ISSN No. 2455-2143, Pages 44-56
Published Online April 2024 in IJEAST (http://www.ijeast.com)

$-r = -r_{NaOH} = k\, C_{NaOH}\, C_{EtAC}$ (2)

The reacting components ethyl acetate, sodium hydroxide, ethanol and water were selected from HYSYS databank, while sodium acetate was hypothesized by means of its molecular weight, normal boiling point and density. Based on considerations that mentioned in property package selection, the property model Peng-Robinson-Stryjek-Vera (PRSV) model catering to real and highly non-ideal (non-electrolytic) chemical systems was selected. The aforementioned reaction was defined in HYSYS by adding a reaction set. The kinetic data were selected from Wijayarathne and Wasalathilake [30], which the activation energy (E_a) and frequency factor (k_o) were found to be 41400 kJ/mol and 2194760.

The average jacket temperature is [31]:

$$T_J = \frac{T_{in} + T_{out}}{2} \quad (3)$$

Taking outlet temperature as a subject:

$$T_{out} = 2T_J - T_{in} \quad (4)$$

The jacket area covers about 80% of the reactor surface, consisting of a flat-end head and a cylindrical shell [31]:

$$A_J = 0.80 \times A_R = 0.80 \times \pi D_o H \quad (5)$$

Thus, the heat that can be transferred to the jacket is:

$$Q_J = U_J A_J (T_J - T_R) \quad (6)$$

The overall heat transfer coefficient, U, is obtained by [32]:

$$\frac{1}{U} = \frac{1}{h_i} + \frac{A_i}{A_o h_o} + \frac{e}{A_i k_m} \quad (7)$$

Where e is the thickness of the reactor wall. The inside film coefficient, h_i, of an agitated vessel is [32]:

$$\frac{h_i D_o}{k} = a\left(\frac{D^2_{Agitator} N\rho}{\mu}\right)^b \left(\frac{c_p \mu}{k}\right)^{1/3} \left(\frac{\mu}{\mu_W}\right)^m \quad (8)$$

Where D_T is diameter of tank, k is thermal conductivity of the process liquid, D_A is diameter of agitator, N is revolutions per second of agitator, ρ is density of process liquid, μ is viscosity of process liquid at temperature in vessel, μ_W is viscosity of process liquid at wall temperature, and c_p is heat capacity of process liquid. For jacket heat transfer coefficient is obtained by Coker [33]:

$$\frac{h_o D_o}{k} = 0.85\left(\frac{D^2_{Agitator} N\rho}{\mu}\right)^{0.66} \left(\frac{c_p \mu}{k_w}\right)^{1/3} \left(\frac{\mu}{\mu_W}\right)^{0.14} \left(\frac{H}{D_o}\right)^{-0.56} \left(\frac{D_{Agitator}}{D_o}\right)^{0.13} \quad (9)$$

Assuming viscosity correction equals 1.0 for water [33]. Thermal conductivity of stainless steel 304 k_w = 14.6 W/m.K [34]. The general form of CSTR energy balance is [35-37]:

$$V_{coil}\rho_{H_2O} cp_{H_2O} \frac{dT}{dt} = v_{H_2O}\rho_{H_2O} cp_{H_2O}(T_{J_{in}} - T_{J_{out}}) + (-\Delta H_R) V_{coil} k C_{NaOH} C_{EtAc} + U_{coil} A_{o_{coil}} (T_R - T_J) + \dot{Q} - \dot{W} \quad (10)$$

At steady-state, the term (dT/dt) equals zero. However, The cooling jacket energy balance is [38]:

$$V_J \rho_{H_2O} cp_{H_2O} \frac{dT_J}{dt} = \dot{m}_{H_2O} cp_{H_2O}(T_{J_{in}} - T_J) + U_J A_J (T_R - T_J) \quad (11)$$

Rearranging and substituting equation (3.40) into equation (3.51), the outlet jacket temperature is:

$$T_{J_{out}} = 2\left(\frac{\dot{m}_w Cp_w T_J^{in} + U_J A_J T_R}{\dot{m}_w Cp_w + U_J A_J}\right) - T_{J_{in}} \quad (12)$$

2. Identification of the Transfer Functions

The transfer functions were identified using System Identification Toolbox, black box model in MATLAB as shown in appendix J. The steps were:

1. MATLAB command window was opened.
2. The dynamic and steady-state data were entered in MATLAB workspace as "input_manVar", "output_manVar", "input_conVar" and "output_conVar", for manipulated variable and controlled variables, respectively.
3. The word "ident" was typed on the command window; a new window titled as "System Identification Tool – Untitled" was appeared.
4. From the box "Import data", "Time domain data…" was selected after click the arrow, a new window smaller titled as "Import window" was appeared.
5. The manipulated variable data (input_manVar and output_manVar) were entered in "Input", and "Output", respectively. Then import icon was clicked.
6. From the box "Estimate", "Process models" was selected in order to find the valve transfer function. After click the arrow new window was appeared, and then estimated icon was clicked after selecting 1 pole and all real models.
7. On data Views area, in the right side of "System Identification" window, a new data titled as "P1" was appeared. This box was dragged to the box labeled as "To workspace" then dropped.
8. In order to entering the controlled data, from the box "Import data", "Time domain data…" was selected after click the arrow, a new window smaller titled as "Import window" was appeared.
9. The controlled variable data (input_conVar and output_conVar) were entered in "Input", and "Output", respectively. Then import icon was clicked.
10. From the box "Estimate", "Process models" was selected in order to find the CSTR transfer function. After click the arrow new window was appeared, and then estimated icon was clicked after selecting 2 poles and all real models.
11. On Model Views area, in the right side of "System Identification" window, a new data titled as "P2" was appeared. This box was dragged to the box labeled as "To workspace" then dropped.

However, all these steps were repeated to get the transfer function for the primary loop.

3. System Stability Techniques

Mathematically, the closed-loop system is stable if all the roots of the characteristic polynomial have negative real parts or if all the poles of the closed-loop transfer function lie in the

International Journal of Engineering Applied Sciences and Technology, 2024
Vol. 8, Issue 12, ISSN No. 2455-2143, Pages 44-56
Published Online April 2024 in IJEAST (http://www.ijeast.com)

left-hand plane (LHP) of the complete plane. The system stability techniques are:

a. The Routh-Hurwitz Stability Criterion

This cirterion provides a convenient method of determining control systems stability. The number of sign changes of this column is equal to the number of roots of the polynomial that are in the (RHP). Thus, for the system to be stable there can be no sign changes in the first column of the Routh array [18, 39].

b. Root-locus Criterion method

Root-locus method is used for finding the roots of the characteristic equation. It determines the roots of the characteristic equation are plotted for all values of a system parameter [18].

c. Bode Criterion Method

Bode curve gives a convenient method to represent the frequency response characteristics of the system to determine the ultimate parameters on semi log plot of the amplitude ratio and phase angle as the frequency is varied from zero to infinity [16, 18].

4. Controller Tuning

Tuning is required to maintain good control, and a rational understanding of the controller form and its behavior is required for effective tuning [40]. The controller tuning objective is to reach a satisfying trade-off between the system criteria, which applies to PID controllers and also any other types of controllers [41]. Table 1, shows the Zirgler-Nichols tuning parameters based on the ultimate gain and period.

Table-1: Ziegler-Nichols Controller Settings [18].

Type of controller	K_p	τ_I	τ_D
P	0.5 K_U	-	-
PI	0.45 K_U	$P_U/1.2$	-
PID	0.60 K_U	$P_U/2.0$	$P_U/8$

III. Results and Discussion

1. Steady-state Simulation

It is assumed to produce a 44,000 kg/year of sodium acetate, with a feed temperature at 39 °C and 1 atmospheric pressure to achieve the conversion required (73.1%) at the flow rates assessed. Fig. 2, shows the entered temperatures, pressures and molar flows for sodium hydroxide and ethyl acetate streams, and the CSTR temperature.

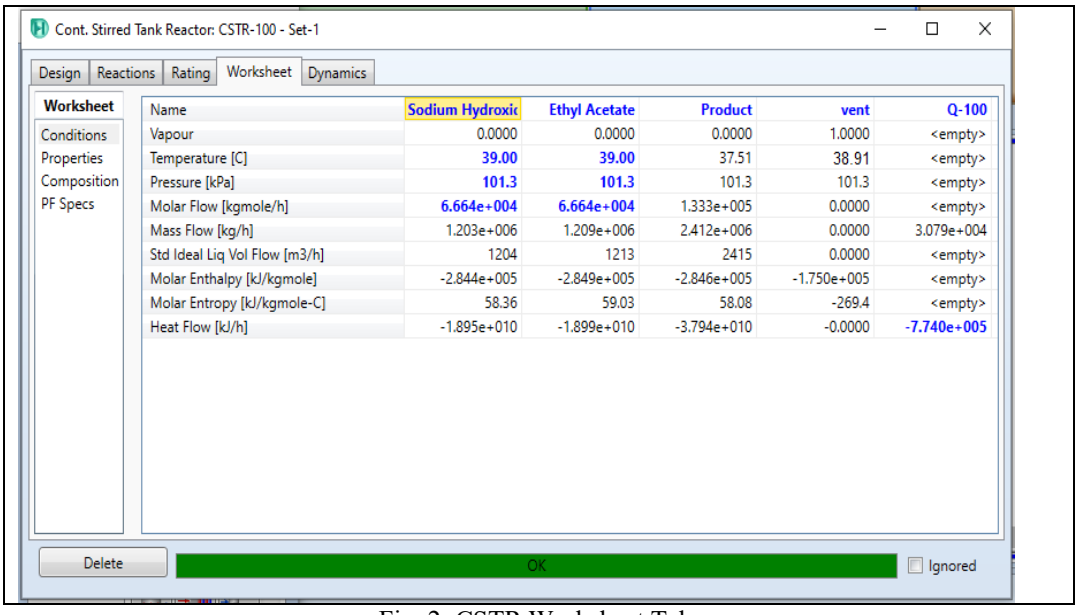

Fig. 2: CSTR Worksheet Tab.

International Journal of Engineering Applied Sciences and Technology, 2024
Vol. 8, Issue 12, ISSN No. 2455-2143, Pages 44-56
Published Online April 2024 in IJEAST (http://www.ijeast.com)

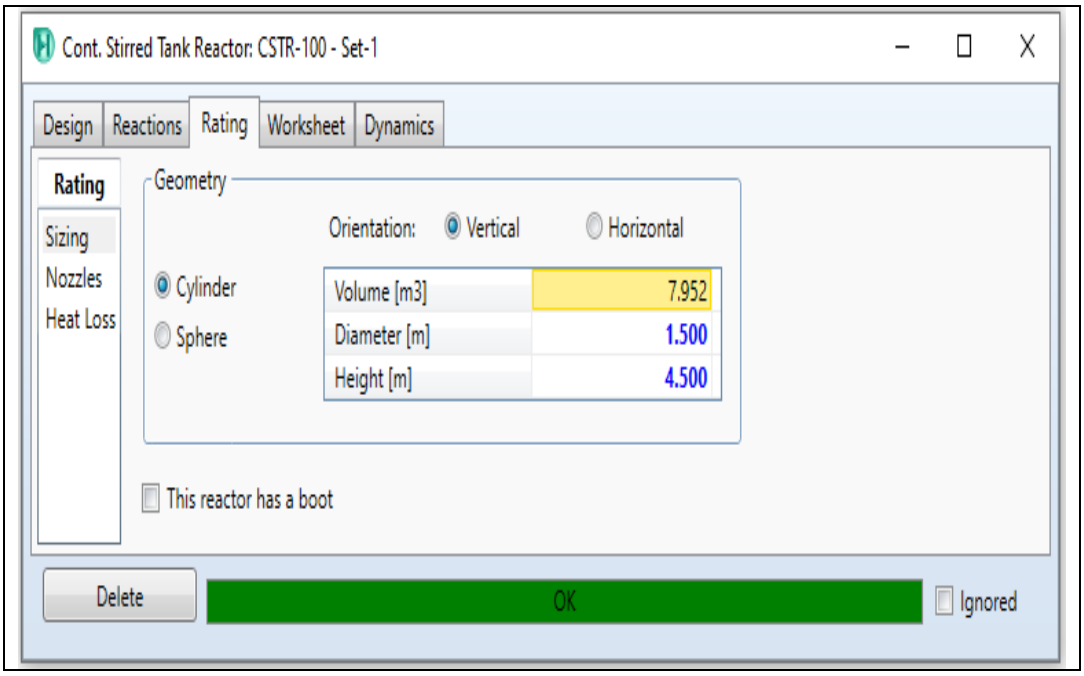

Fig. 3: CSTR Dimension in Rating Tap.

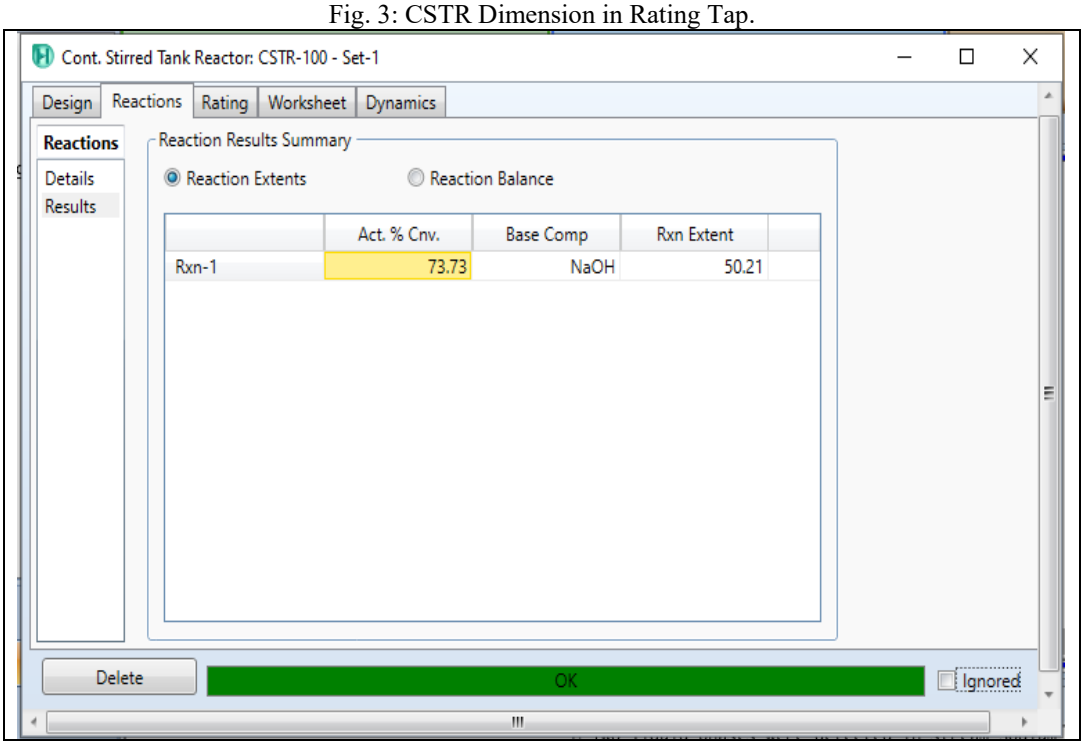

Fig. 4: Reaction Results Tap from HYSYS Software.

From fig. 3, CSTR volume is 7.952 m^3, which is typically the desired scale-up volume. The simulated reaction conversion was obtained as 73.73%, with percentage error of 0.87% from experimental reaction conversion as shown in fig. 4.

2. Dynamic-state Simulation

The flow sheet of ethyl acetate hydrolysis was adjusted at dynamic-mode to meet the stream flow and pressure specifications. This adjustment was done by adding valves and activating pressure specifications in material streams in order to obtain the dynamic-mode requirements as shown in fig. 5.

International Journal of Engineering Applied Sciences and Technology, 2024
Vol. 8, Issue 12, ISSN No. 2455-2143, Pages 44-56
Published Online April 2024 in IJEAST (http://www.ijeast.com)

The dynamic data of the controlled variables and the steady-state data of the manipulated variables are shown in figures 6, 7 and 8, respectively. Figures 6 and show the change in CSTR temperature and outlet cooling water temperature with step change response of cooling water volumetric flow rate. Fig. 8, shows the change in valve opening (%) with cooling water volumetric flow rate.

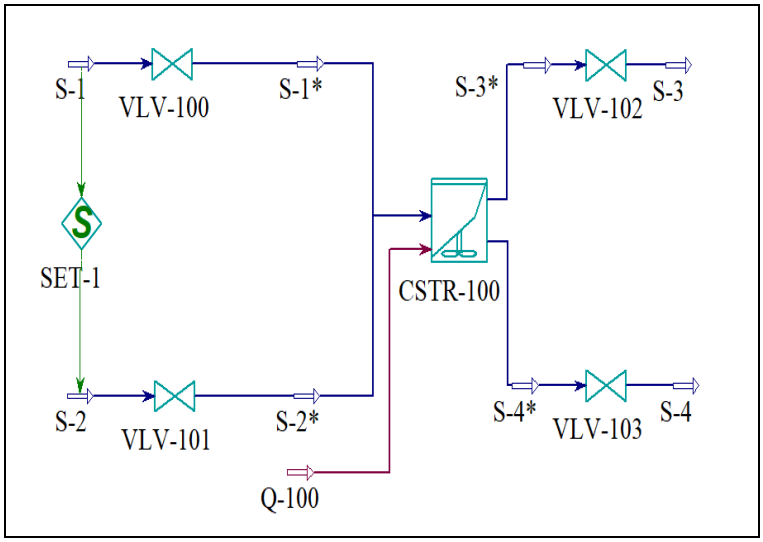

Fig. 5: CSTR Flow Sheet in Aspen HYSYS Simulation Environment.

From fig. 6, the volumetric flow rate of cooling water was changed from 0.16 to 0.34 m^3/min in dynamic mode to examine its response on the CSTR temperature. The change in reactor temperature was observed in changing from 39.3 °C, and gradually increased until the reactor temperature riched to 30.1 °C at 250 min. It has been recorded 416 data point for both the temperature of the CSTR and the outlet cooling water temperature in dynamic mode. In figures 7 and 8, the response of valve opening (%) on volumetric flow rate of cooling water utility was examined in dynamic-state mode. The step change from 50% to 100% of the valve opening, and the response of the cooling water volumetric flow rate was from 0.16 to 0.33 m^3/min. It has been recorded 416 data point for mole fraction of sodium acetate with the mass flow rate of cooling water.

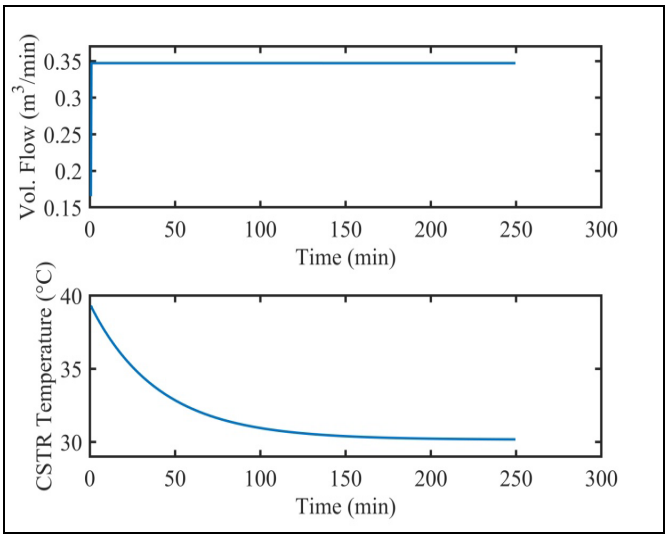

Fig. 6: Response of CSTR Temperature with Cooling Water Volumetric Flow Rate Step Change.

International Journal of Engineering Applied Sciences and Technology, 2024
Vol. 8, Issue 12, ISSN No. 2455-2143, Pages 44-56
Published Online April 2024 in IJEAST (http://www.ijeast.com)

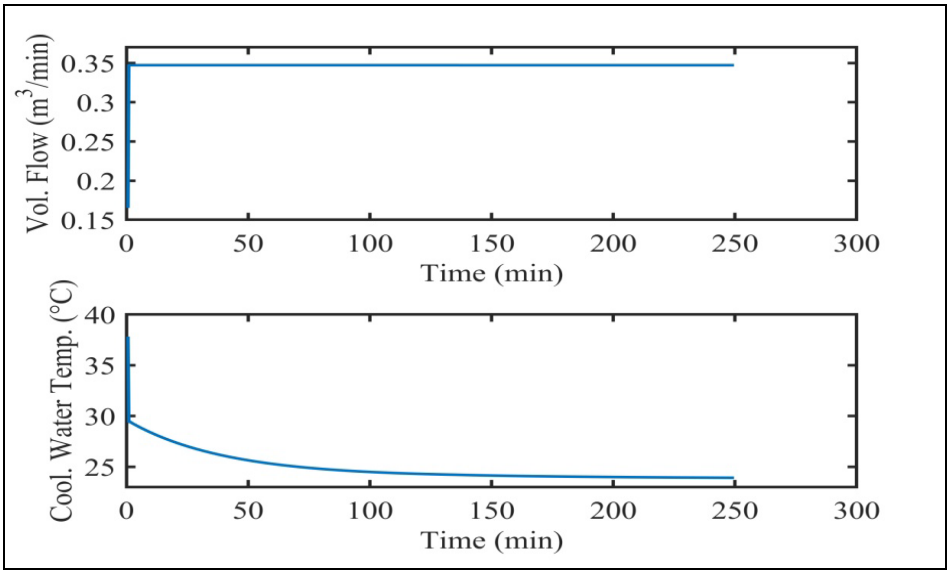

Fig. 7: Response of Cooling water Temperature with Cooling Water Volumetric Flow Rate Step Change.

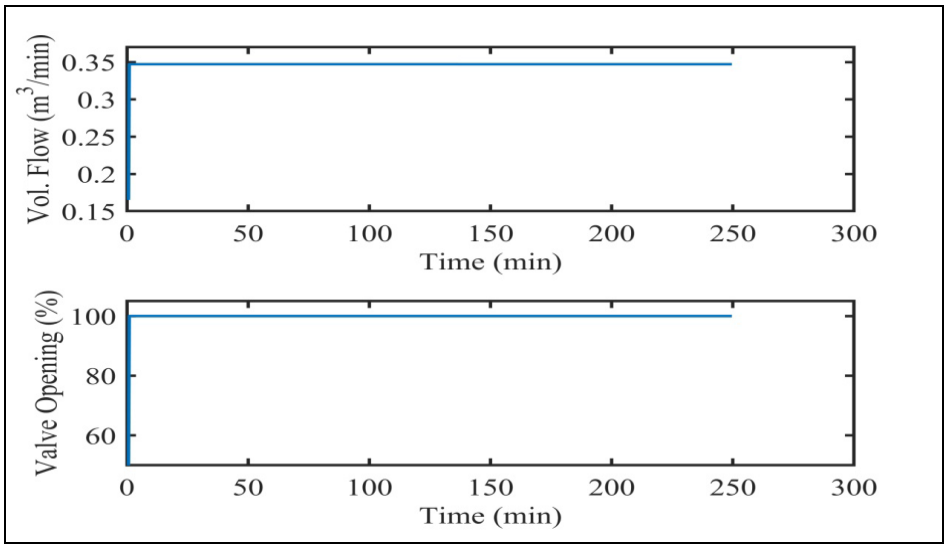

Fig. 8: Response of Cooling Water Volumetric Flow Rate with Valve Opening step change.

3. Identification of the Transfer Functions of the System

Using System Identification tool in MATLAB, the transfer function for the process, and the valve element are, respectively:

$$G_{p_1} = \frac{0.07452}{(0.87s+1)(0.15s+1)}$$

$$G_{p2} = \frac{1.353}{(0.04946s+1)(0.052483+1)}$$

$$G_v = \frac{2.8}{25.67s+1}$$

In HYSYS, it assumed the controller is perfectly accurate in its measurement of the process variable [42]. Thus, the transfer function of the measuring element is:

$G_{m_1} = 1$

$G_{m_2} = 1$

Therefore, fig. 9 showed the cascade feedback control system for the CSTR with block diagrams of process, valve and measuring element.

International Journal of Engineering Applied Sciences and Technology, 2024
Vol. 8, Issue 12, ISSN No. 2455-2143, Pages 44-56
Published Online April 2024 in IJEAST (http://www.ijeast.com)

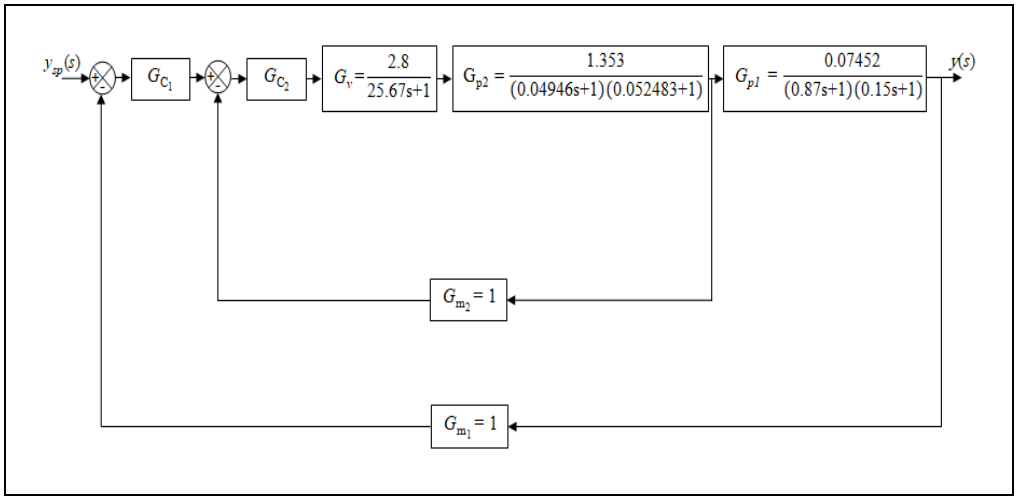

Fig. 9: Cascade Control Strategy Block Diagram for CSTR Temperature Control.

4. Routh-Hurwitz Criterion for Secondary Loop

In order to get the ultimate gain of the secondary loop, the characteristic equation when using P-controller for the loop:

$$0.06663\ s^3 + 2.619\ s^2 + 25.77\ s + \left(1 + 3.788k_{C_2}\right) = 0$$

Routh array: number of rows= n + 1 = 3 + 1 = 4

s^3	0.06663	25.77
s^2	2.619	$\left(1 + 3.788k_{C_2}\right)$
s	b_1	0
s^0	c_1	0

where:

$b_1 = 25.744 - 0.0964k_{C_2}$

$b_2 = 0$

$c_1 = \left(1 + 3.788k_{C_2}\right)$

$c_2 = 0$

However, Routh array becomes:

s^3	0.06663	25.77
s^2	2.619	$\left(1 + 3.788k_{C_2}\right)$
s	$25.744 - 0.0964k_{C_2}$	0
s^0	$\left(1 + 3.788k_{C_2}\right)$	0

At ultimate gain, $= K_U$, $b_1 = 0$

$0 = 25.744 - 0.0964K_U$

$$K_U = \frac{25.744}{0.0964} = 267.05$$

Checking system stability using Routh array by substituting the value of k_C using Ziegler-Nichols tuning method in Routh array

$k_{C_2} = 0.5 \times K_U = 0.5 \times 267.05 = 133.5$

Routh array becomes:

s^3	3.35	26.31
s^2	2.619	506.698
s^1	12.875	0
s^0	506.698	0

Since $0 < k_{C2} < \infty$, all elements of the first column were positive and there is no change of sign, and all roots of the characteristic equation lie on LHP. Whereby, the system is stable for all values of k_{C2}, and then a large value for the gain can be used which produces a very fast closed loop response.

5. Tuning of Controllers for Primary Loop

The ultimate parameters were determined using a Simulink simulation environment for the primary closed-loop transfer function with P-action controller as an adjustable gain as shown in fig. 10.

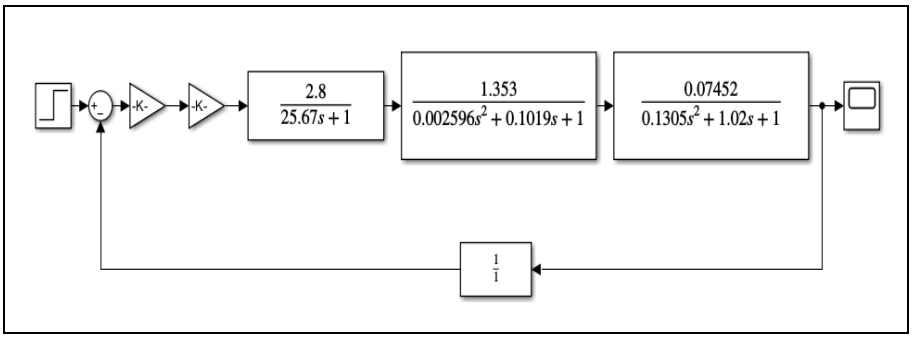

Fig. 10: Simulink Block Diagram for Secondary Closed-loop.

International Journal of Engineering Applied Sciences and Technology, 2024
Vol. 8, Issue 12, ISSN No. 2455-2143, Pages 44-56
Published Online April 2024 in IJEAST (http://www.ijeast.com)

The trials to estimate the ultimate gain when the controller is proportional shown in figures 11 to 13 below:

- The first trial (K = 3.15)

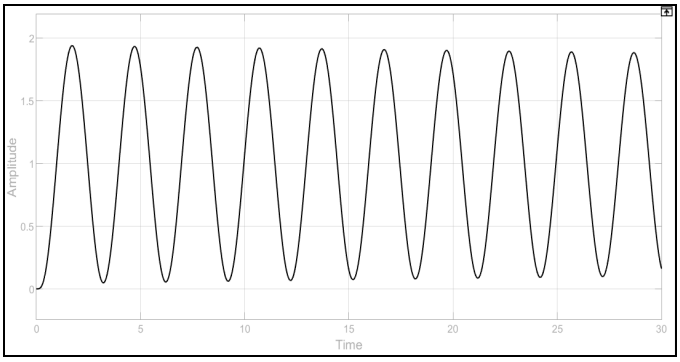

Fig. 11: The First Trial for Primary Closed-loop.

- The second trial (K = 3.20)

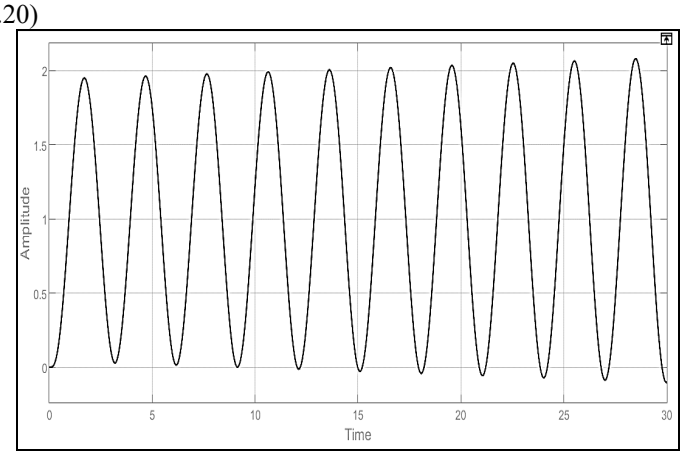

Fig. 12: The Second Trial for Primary Closed-loop.

- Third trial estimated the ultimate gain (= K_U = 3.17)

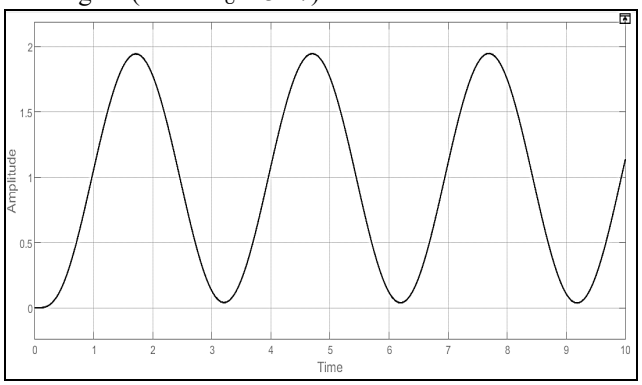

Fig. 13: Z-N Tuning Plot for P-controller at Critical Stable for Primary Closed-loop.

From figures 11 and 12, the response of the secondary colosd-loop system is oscillates and unstable. Fig. 13, shows the response of a marginally stable system. It is a pure harmonic response, in which the period of oscillation P_U can be measured. However, the ultimate gain (K_U) is 3.17.

International Journal of Engineering Applied Sciences and Technology, 2024
Vol. 8, Issue 12, ISSN No. 2455-2143, Pages 44-56
Published Online April 2024 in IJEAST (http://www.ijeast.com)

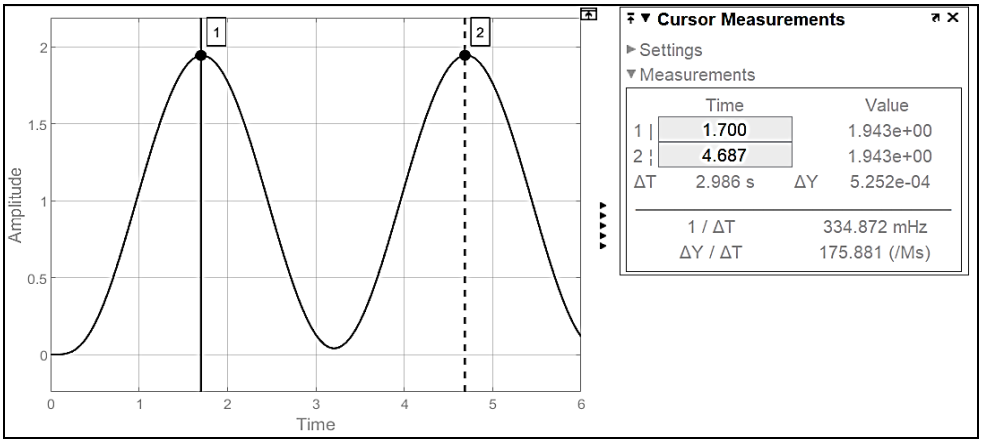

Fig. 14: Measuring the Ultimate Peak for Secondary Closed-loop.

The "Cursor Measurement" was used to the sustained oscillation, and the points (1) and (2) were adjusted to the peaks as shown in fig. 14. The ultimate period (P_U) was determined as 2.986 sec in "Measurements" screen.

Using Ziegler-Nichols table to calculate the controller parameters, the values of these parameters are shown in table 2.

Table-2: The Adjustable Parameter of the Controller of the Primary Loop.

Type of controller	K_p	τ_I **(sec)**	τ_D **(sec)**
P	1.585	-	-
PI	1.427	2.488	-
PID	1.902	1.493	0.373

6. Root Locus Criterion for Primary Loop

Fig. 15, showed the Root-locus plot for the closed-loop system. The root locus plot lies completely on the LHP of complex plane; system is stable for all values of k_C. From fig. 15, the cross-over frequency, the ultimate gain and the ultimate period are, respectively:

$\omega_{CO} = 2.11$ rad/sec

$K_U = 2.19$

$P_U = 2\pi/\omega_{CO} = 2.98$ sec

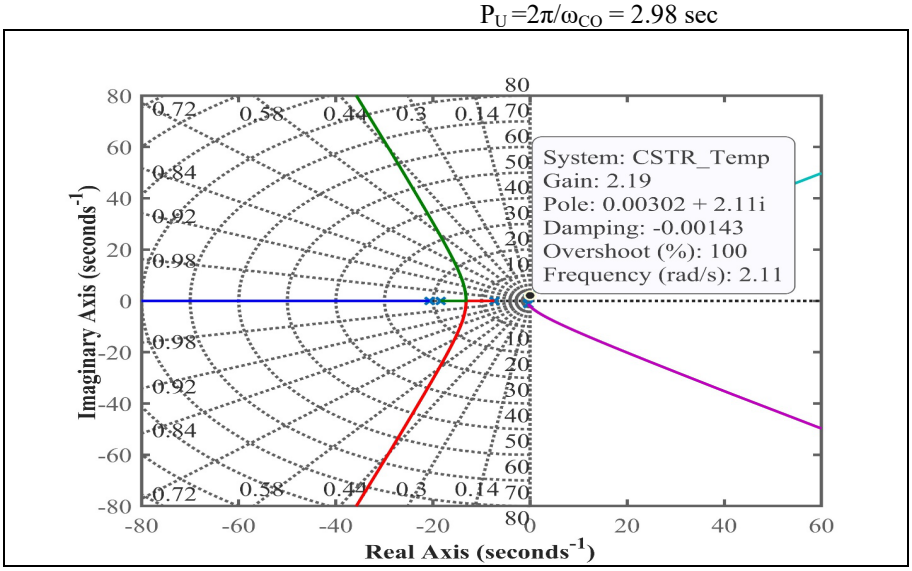

Fig. 15: Root-locus Plot for the Primary-loop.

International Journal of Engineering Applied Sciences and Technology, 2024
Vol. 8, Issue 12, ISSN No. 2455-2143, Pages 44-56
Published Online April 2024 in IJEAST (http://www.ijeast.com)

7. Bode Stability Criterion for Primary Loop

Bode plot for the primary loop is shown in fig. 15. The system was stable up to -180 at the cross over frequency (ω_{CO}). At phase angle = -180°, Amplitude Ratio AR = 0.463 abs

$$K_U = \frac{1}{AR} = \frac{1}{0.463} = 2.16$$

Cross over frequency ω_{CO} = 2.11 rad/sec

P_U = 2.98 sec

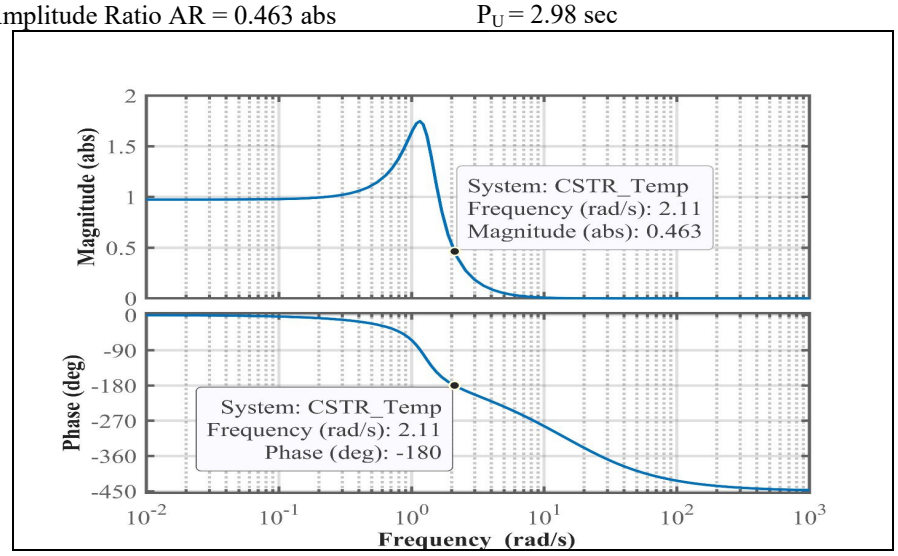

Figure (4.27): Bode Diagram for the Primary-loop.

8. System Response with P, PI and PID Control for Primary Loop

Finally, in order to compare the response of P, PI and PID Controllers of the system, fig. 16, showed the step responses of all controllers in unit step change response simulation.

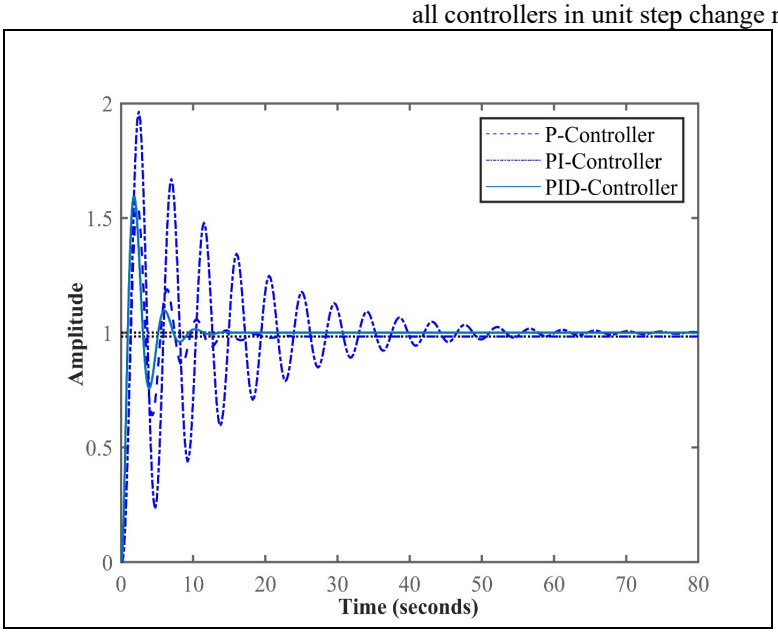

Fig. 16: Step Change Response Using P, PI and PID Controllers for Primary Loop.

Table-3: Summary of Characteristics of the Step Responses of P, PI and PID Controllers for Primary Loop.

Controller	Rise time (sec)	Settling time (sec)	Overshoot (%)	Final value
P	0.783	15.1	58.3	0.984
PI	0.763	54.6	96.3	1.000
PID	0.591	8.89	59.7	1.000

From fig. 16 and table 3, it can be seen that the P and PID controller have improved the performance of the system over the PI controller. PI controller has a highest overshoot ratio and longest settling time, while PID controller has a lowest overshoot and the shortest settling and rise times. While the P controller response showed the deviation from the desired final value that gave minimum overshoot with best performance was selected is a PID-controller for the primary closed-loop.

IV.CONCLUSION

The steady-state and dynamic data are used for identifying the system transfer functions, analyzing the system stability and determining the adjustable parameters for cascade tepmerature control system.

There are many methods that are used to get the adjustable parameters such as Routh-Hurwitz, Direct substitution and there are another three graphical method, Bode, Nyquist, and root locus. Ziegler-Nicholas criterion is used to tune the adjustable parameters for both secondary and primary loops.

PID controller for the primary loop provides the highest gain than P and PI controllers. Meanwhile, PI controllers provide the higest overshoots than P and PID controllers. Whereby, the PID-controller gave performance for the primary closed-loop.

V. REFERENCES

[1]. Antonelli, R., and Astolfi, A. (2003). Continuous Stirred Tank Reactors: Easy to Stabilise? Automatica, 39(10), pp. 1817-1827.

[2]. Zhao, D., Zhu, Q., and Dubbeldam, J. (2015). Terminal Sliding Mode Control for Continuous Stirred Tank Reactor. Chemical Engineering Research and Design, 94, pp. 266-274.

[3]. Kumar, M., and Singh, R. (2016). Comparison of Non-linear, Linearized 2nd Order and Reduced to FOPDT Models of CSTR using Different Tuning Methods. Resource-Efficient Technologies, 2, pp. S71-S75.

[4]. Wallam, F., and Memon, A. Y. (2017). A Robust Control Scheme for Nonlinear Non-isothermal Uncertain Jacketed Continuous Stirred Tank Reactor. Journal of Process Control, 51, pp. 55-67.

[5]. Tandon, B., Narayan, S., and Kumar, J. (2018). Nonlinear Disturbance Observer Based Robust Control for Continuous Stirred Tank Reactor. ICIC Express Letters, 12(1), pp. 1-7.

[6]. Aris, R., and Amundson, N. R. (1958). An Analysis of Chemical Reactor Stability and Control—I: The Possibility of Local Control, with Perfect or Imperfect Control Mechanisms. Chemical Engineering Science, 7(3), pp. 121-131.

[7]. Uppal, A., Ray, W., and Poore, A. (1974). On the Dynamic Behavior of Continuous Stirred Tank Reactors. Chemical Engineering Science, 29(4), pp. 967-985.

[8]. Morari, M., and Zafiriou, E. (1987). Robust Process Control. Chemical Engineering Research and Design, 65(6), pp. 462-479.

[9]. Hoo, K. A., and Kantor, J. C. (1985). An Exothermic Continuous Stirred Tank Reactor is Feedback Equivalent to a Linear System. Chemical Engineering Communications, 37(1-6), pp. 1-10.

[10]. Kravaris, C., and Chung, C. B. (1987). Nonlinear State Feedback Synthesis by Global Input/output Linearization. AIChE Journal, 33(4), pp. 592-603.

[11]. Alvarez, J., Alvarez, J., and González, E. (1989). Global Nonlinear Control of a Continuous Stirred Tank Reactor. Chemical Engineering Science, 44(5), pp. 1147-1160.

[12]. Doyle III, F. J., Packard, A. K., and Morari, M. (1989). Robust Controller Design for a Nonlinear CSTR. Chemical Engineering Science, 44(9), pp. 1929-1947.

[13]. Limqueco, L., and Kantor, J. (1990). Nonlinear Output Feedback Control of an Exothermic Reactor. Computers & Chemical Engineering, 14(4-5), pp. 427-437.

[14]. Alvarez-Ramírez, J. (1994). Stability of a Class of Uncertain Continuous Stirred Chemical Reactors with a Nonlinear Feedback. Chemical Engineering Science, 49(11), pp. 1743-1748.

[15]. Dochain, D. (1994). Design of Adaptive Linearizing Controllers for Non-isothermal Reactors. International Journal of Control, 59(3), pp. 689-710.

[16]. Salih, G. M., and Abdalla, G. A. G. (2022). Control and Simuiate of Liquid Liquid Extraction Column. International Journal of Engineering Applied Sciences and Technology (ijeast), 7(6), pp. 306-310.

[17]. Ahmed, A., Gasmelseed, G., Karama, A., and Musa, A. (2013). Cascade Control of a Continuous Stirred Tank Reactor (CSTR). Journal of Applied and Industrial Sciences, 1(4), pp. 16-23.

[18]. Gasemseed, G. A. (2013). A Textbook of Chemical Engineering Process Control. Khartoum, Sudan: G-Town Center.

[19]. Oravec, J., Bakošová, M., Hanulová, L., and Mészáros, A. (2018). Multivariable Robust Model Predictive Control of a Laboratory Chemical Reactor, Computer Aided Chemical Engineering, 43, pp. 961-966.

[20]. Javinsky, M. A., and Kadlec, R. H. (1970). Optimal Control of a Continuous Flow Stirred Tank Chemical Reactor. AIChE Journal, 16(6), pp. 916-924.

[21]. Mungcharoen, T., and Onifade, K. (2000). Mathematical Modeling and Computer Simulation of a Tubular Flow Reactor. AU Journal of Technology, 3(4), pp.181-188.

[22]. Djaeni, M., Suherman, Jalasanti, K., and Mukti, R. R. (2001). Control System Strategy Of The Saponification Process Between Ethyl Acetate And Sodium Hydroxide. Reaktor, 5(2), pp. 54-58.

[23]. Mousa, K. M., and Dawood, Z. E. (2015). Study on Control of CSTR Using Intelligent Strategies. Al-Nahrain University, College of Engineering Journal (NUCEJ), 18(2), pp. 294-303.

[24]. Mousa, K. M., and Dawood, Z. E. (2015). Study on Control of CSTR Using Intelligent Strategies. Al-Nahrain University, College of Engineering Journal (NUCEJ), 18(2), pp. 294-303.

[25]. Türkşen, Ö., and Ertunç, S. (2015). Optimization of Saponification Process in Multi-response Framework by using Desirability Function Approach. Sakarya University Journal of Science, 19(2), pp. 141-149.

[26]. Zare, K. B., Sunil, R. S., and Anil, M. S. (2017). Modelling and Simulation of Saponification Reaction in Different Type of Reactor. International Journal of Advanced Technology in Engineering and Science, 5(4), pp. 324-332.

[27]. Deifalla, M. H. H. (2020). Simulation and Control of CSTR for Ethyl Acetate Hydrolysis Using Aspen HYSYS and MATLAB. M.Sc Thesis, University of Science and Technology, Sudan.

[28]. Mukhtar, A., Shafiq, U., Qazi, M., Qadir, H., Qizilbash, M., and Awan, B. (2017). Kinetics of Alkaline Hydrolysis of Ethyl Acetate by Conductometric Measurement Approach over Temperature Ranges (298.15-343.15 K). Austin Chemical Engineering, 4(1), pp. 1046.

[29]. Wijayarathne, U., and Wasalathilake, K. C. (2014). Aspen Plus Simulation of Saponification of Ethyl Acetate in the Presence of Sodium Hydroxide in a Plug Flow Reactor. International Journal of Chemical and Molecular Engineering, 8(10), pp. 1089-1096.

[30]. Wijayarathne, U., and Wasalathilake, K. (2014). Aspen Plus Simulation of Saponification of Ethyl Acetate in the Presence of Sodium Hydroxide in a Plug Flow Reactor. Journal of Chemical Engineering & Process Technology, 5(6), pp. 1-8.

[31]. Silla, H. (2003). Chemical Process Engineering: Design and Economics. New York, USA: Marcel Dekker, Inc, pp. 332-335.

[32]. Luyben, W. L. (2007). Chemical Reactor Design and Control. USA: John Wiley & Sons, Inc, pp. 40.

[33]. Coker, A. K. (2001). Modeling of Chemical Kinetics and Reactor Design. USA: Gulf Professional Publishing, pp. 620.

[34]. Chen, H., Frankel, J. I., and Keyhani, M. (2017). Nonlinear Inverse Heat Conduction: Digitally Filtered Space Marching with Phase-plane and Cross-correlation Analyses. Numerical Heat Transfer, Part B: Fundamentals, 72(2), pp. 109-129.

[35]. Seborg, D. E., Edgar, T. F., Mellichamp, D. A., and Doyle III, F. J. (2017). Process Dynamics and Control (4th ed.). USA: John Wiley & Sons, pp. 26-27.

[36]. Kravaris, C., and Chung, C. B. (1987). Nonlinear State Feedback Synthesis by Global Input/output Linearization. AIChE Journal, 33(4), pp. 592-603.

[37]. Duque, A., and Ochoa, S. (2019). A Comparison of Control Architectures for Controlling a CSTR for Acrylic Acid Production. Paper presented at the 2019 IEEE 4th Colombian Conference on Automatic Control (CCAC), pp. 1-6.

[38]. Roffel, B., and Betlem, B. H. (2004). Advanced Practical Process Control. USA: Springer-Verlag Berlin Heidelberg GmbH, pp. 97.

[39]. Abu-Goukh, M. E. (2014). Controlling Techniques and System Stability. Khartoum, Sudan: Sudan Currency Printing Press.

[40]. Liptak, B. G. (2018). Instrument Engineers' Handbook, Volume two: Process Control and Optimization. USA: CRC press, pp. 124.

[41]. Blondin, M. J. (2021). Controller Tuning Optimization Methods for Multi-Constraints and Nonlinear Systems: A Metaheuristic Approach. Swizerland: Springer Nature Swizerland AG, pp. 2.

[42]. Aspen-Hysys. (2005). Simulation Basis. Cambridge, United States: Aspen Technology, Inc, pp. 3-20.